Pharm Res (2012) 29:1270–1281
DOI 10.1007/s11095-011-0663-7

RESEARCH PAPER

Force Dependent Internalization of Magnetic Nanoparticles Results in Highly Loaded Endothelial Cells for Use as Potential Therapy Delivery Vectors

Cristin MacDonald • Kenneth Barbee • Boris Polyak

Received: 16 August 2011 / Accepted: 20 December 2011 / Published online: 11 January 2012
© Springer Science+Business Media, LLC 2012

ABSTRACT

Purpose To investigate the kinetics, mechanism and extent of MNP loading into endothelial cells and the effect of this loading on cell function.

Methods MNP uptake was examined under field on/off conditions, utilizing varying magnetite concentration MNPs. MNP-loaded cell viability and functional integrity was assessed using metabolic respiration, cell proliferation and migration assays.

Results MNP uptake in endothelial cells significantly increased under the influence of a magnetic field *versus* non-magnetic conditions. Larger magnetite density of the MNPs led to a higher MNP internalization by cells under application of a magnetic field without compromising cellular respiration activity. Two-dimensional migration assays at no field showed that higher magnetite loading resulted in greater cell migration rates. In a three-dimensional migration assay under magnetic field, the migration rate of MNP-loaded cells was more than twice that of unloaded cells and was comparable to migration stimulated by a serum gradient.

Conclusions Our results suggest that endothelial cell uptake of MNPs is a force dependent process. The *in vitro* assays determined that cell health is not adversely affected by high MNP loadings, allowing these highly magnetically responsive cells to be potentially beneficial therapy (gene, drug or cell) delivery systems.

C. MacDonald · K. Barbee · B. Polyak
School of Biomedical Engineering, Drexel University
Philadelphia, Pennsylvania 19104, USA

B. Polyak (✉)
Department of Surgery, Drexel University College of Medicine
245 N. 15th Street, NCB Suite 7150, Mail Stop 413
Philadelphia, Pennsylvania 19102, USA
e-mail: bpolyak@drexelmed.edu

KEY WORDS cell targeting · cell therapy · endocytosis · magnetic cell loading · magnetic nanoparticles

ABBREVIATIONS

BAEC	bovine aortic endothelial cell
DLS	dynamic light scattering
FBS	fetal bovine serum
MNP	magnetic nanoparticles
PBS	phosphate buffered saline
PLA	poly(lactic acid)
PVA	poly(vinyl alcohol)

INTRODUCTION

Nanotechnology is of continuously growing interest in biomedicine, and magnetic nanoparticles (MNPs) are at the center of this research (1–3). Currently, MNPs have been shown to be useful in gene (4–10), drug (11–15), cell delivery (16–19), imaging and diagnostics (20), with the main application being their use as contrast agents in Magnetic Resonance Imaging (MRI) (21). Aside from these standard purposes, magnetic nanoparticles are an attractive option for drug delivery due to the ease of surface functionalization and biocompatibility (20).

Cells loaded with MNPs as vectors for targeted therapy delivery can potentially eliminate the difficulties of circumventing the immune system of the human body (22,23). Previous work has shown that MNPs and MNP-loaded endothelial cells are promising vectors for targeted delivery to cardiovascular stents (17,24,25). Many groups have analyzed the endocytotic mechanisms used for nanoparticles to enter cells (26–29), and MNP entry into cells has long been demonstrated to increase gene transfection in

cells (16,30–32). However, MNP-enhanced gene transfection papers measure the amount of transfection achieved, not the number of particles that have been loaded into the cell. The purpose of this study was to examine how a static magnetic field influences MNP uptake into endothelial cells and to quantify loading of these MNPs under various conditions.

For most cell-targeting applications, it is desirable to load cells with the greatest amount of magnetic nanoparticles possible, thereby maximizing the magnetic responsiveness of the cell, without causing toxicity or other harmful effects to the cell. The ability to quantify the number of MNPs taken into cells is essential for obtaining this optimal loading. Our goal was to show that we can highly load endothelial cells and retain similar cytoskeletal function and viability as standard control cells.

Finally, our study examined whether a magnetic field can influence the migration of MNP-loaded cells in a 3-D migration system. We show that the application of a magnetic field can significantly enhance the migration of these highly MNP-loaded cells through a type-I collagen coated synthetic membrane. This study represents a first step in the characterization of the feasibility of magnetically loaded cell transport through soft tissues.

MATERIALS AND METHODS

Materials

Poly(D,L-lactide) (average M_w: 75–120 kD), ferric chloride hexahydrate, ferrous chloride tetrahydrate, sodium hydroxide, oleic acid, and polyvinyl alcohol (87–90% hydrolyzed, average M_w: 30–70 kD), N-Hydroxysuccinimide (NHS), N,N′-Diisopropylcarbodiimide (DIC), Cytochalasin-D were obtained from Sigma-Aldrich (St. Louis, MO, USA). Poly(D,L-lactide) 100DL 4A (acid end, M_w: 54 kD, M_n: 34 kD) was obtained from Lakeshore Biomaterials (Birmingham AL, USA). BODIPY®TR cadaverine (588/617), Live/Dead Viability Cytotoxicity staining kit and Cell-Trace™ Calcein Green were purchased from Life Technologies™ (Carlsbad, CA, USA). Polylactide covalently labeled with BODIPY® 564/570 (Life Technologies™) was a generous gift of Dr. Robert Levy from the Children's Hospital of Philadelphia. All solvents were obtained from Fisher Scientific (Pittsburgh, PA, USA) and were of HPLC grade. Deionized water used in all experimental procedures was obtained using a Milli-Q water purification system. Glass fiber 1.0 μm and 5.0 μm syringe driven filters were purchased from Millipore (Millipore, Bedford MA, USA). Phosphate buffered solution (PBS) and Dulbecco's modified eagle's medium (DMEM) supplemented with L-Glutamine, 4.5 g/L Glucose and Sodium Pyruvate was from MediaTech (Manassas VA, USA), BenchMark™ heat inactivated fetal bovine serum (FBS) was obtained from Gemini Bio-Products (West Sacramento, CA USA), Alamar Blue was purchased from AbD Seroteck (Kidlington, UK). Fluoroblok transwell inserts with 8 μm pores were purchased from VWR (Radnor, PA, USA).

Methods

Magnetic Nanoparticle Formulation

Magnetite was obtained from ferric and ferrous chloride by alkaline precipitation as previously described (33). In brief, for 10% MNP, 65 and 24 mg of ferric and ferrous chloride were dissolved in 9.04 mL of water and precipitated with 0.96 mL of 1 N NaOH; for 30% MNP, 195 and 72 mg of ferric and ferrous chloride were dissolved in 7.12 mL of water and precipitated with 2.88 mL of 1 N NaOH; for 50% MNP, 455 and 168 mg of ferric and ferrous chloride were dissolved in 3.28 mL of water and precipitated with 6.72 mL of 1 N NaOH. Precipitated magnetite in each formulation was magnetically separated, washed twice with degassed DI water, re-suspended in 2 mL of ethanol, and coated with 200 mg oleic acid with heating under argon to 90°C in a water bath for 10 min. Excess oleic acid was phase-separated by drop-wise addition of 4 mL of water and the lipid-coated magnetite was washed twice with ethanol to remove the excess of the oleic acid. In this study, we examined the effect of various magnetite loadings within the (poly)lactic acid (PLA) matrix on cellular uptake of magnetic PLA-based nanoparticles. For this purpose, various amounts of lipophilic magnetite (28, 84 and 196 mg, obtained as described above) were dispersed in 6 mL of chloroform, forming stable magnetic fluids further used for magnetic nanoparticle preparation. The above amounts of magnetite were calculated based on the input amount of iron salts to result in 12.2% (ca. 10%), 29.6% (ca. 30%) and 49.5% (ca. 50%) (w/w) theoretical magnetite loadings within PLA matrix. Polylactide (PLA)-based magnetite-loaded nanoparticles (MNPs) were prepared by the modified emulsification-solvent evaporation method as described elsewhere (11,33). Fluorescent PLA-based magnetic particles were formulated by dissolution of 180 mg of non-labeled PLA and 20 mg of fluoresecently labeled (BODIPY®TR (588/617) or BODIPY® (564/570) PLA in 6 mL of magnetic fluid (containing various amounts of magnetite) to form an organic phase. The organic phase was emulsified in 15 mL of pre-chilled 1.5% (w/v) polyvinyl alcohol (PVA) by sonication, and the organic solvents were removed by evaporation under reduced pressure at 30°C. The particles obtained were passed through a 1.0 μm glass fiber and lyophilized with 10% (w/v) trehalose as a cryoprotectant.

Lyophilized MNPs were kept at +4°C in 100 μL aliquots and re-suspended in deionized water before use.

Fluorescently Labeled PLA

Carboxyl end groups of PLA were coupled with amine-containing BODIPY® TR cadaverine (588/617) using carbodiimide chemistry in organic medium. The carboxyl group activation step was carried out in methylene chloride using NHS/DIC at a 1:1 molar ratio to obtain succinimidyl ester of PLA (PLA-Su). The molar ratio of NHS/DIC to PLA was kept at 300. The activated PLA-Su was precipitated three times from methylene chloride into cold methanol. In the next step, the PLA-Su was coupled with BODIPY® TR cadaverine (588/617) under argon atmosphere for 24 h at basic conditions in methylene chloride supplemented with triethylamine. The excess of base was neutralized with acetic anhydride and the fluorescently labeled PLA was precipitated three times from methylene chloride into cold methanol.

MNP Characterization

Particle size and zeta-potential measurements were determined by dynamic light scattering (DLS) using a Zetasizer NanoZS equipped with 632.8 nm laser (Malvern, UK). The magnetic properties of MNPs and MNP-loaded cells were measured by an alternating gradient magnetometer (Princeton Instruments Corporation, Princeton, NJ, USA). The magnetite content of MNPs was determined spectrophotometrically (using Synergy^{TM} 4 multimode plate reader, BioTek Instruments, Inc. Winooski, VT, USA and UV compatible 96-well plates, BD Bioscienses, Franklin Lakes, NJ, USA) in 1N hydrochloric acid (λ=335 nm) against a standard curve after MNP degradation with 1N aqueous sodium hydroxide (90°C, 30 min) and dissolution of the iron containing precipitate in the acid solution.

Magnetic Nanoparticle Uptake

Bovine Aortic Endothelial cells (BAECs) were seeded on clear-bottom 96-well plates at a density of 2.0×10^4cells per well by using DMEM supplemented with 10% FBS and grown until confluence. Dry aliquots of 10%, 30% and 50% (w/w) iron oxide-loaded PLA-based MNPs were re-suspended in 100 μL of deionized water, and 20 μL (equivalent to ~0.30 mg of dry weight 10% loaded MNP, ~0.38 mg of dry weight 30% loaded MNP and ~0.53 mg of dry weight 50% loaded MNP) of the original nanoparticle suspension was diluted into 10 mL of 10% FBS supplemented DMEM. This MNP suspension was filtered through a Millipore syringe driven filter with 5.0 μm pores in order to separate any aggregates of MNPs. To reduce variability in endocytotic activity, the cells were synchronized with respect to cell cycle activity by incubating at 4°C for 30 min. Then MNPs were added to cells at different doses (100, 75, 50 and 25% of the initial dilution as described above), and cell cultures were incubated at 37°C on a 96-well magnetic separator with an average surface field of 500 Gauss and field gradient of 32.5 T/m as a magnetic field source (LifeSep 96F, Dexter Magnetic Technologies, Fremont, CA). The control (non-magnetic condition) cells were incubated off the magnet. Further, at predetermined time points of 2, 4, 6, 8, 10 and 24 h, cells were washed with PBS, and the amount of internalized MNPs was measured fluorimetrically ($\lambda_{em}/\lambda_{ex}$=588/618 nm) using a Synergy^{TM} 4 reader (BioTek Instruments, Inc.). The total dose of MNPs initially given to cells was measured at each time point before the washing step. Cell viability was determined after 12 h of MNP uptake by using Calcein Green staining and the Alamar Blue assay as described by the manufacturer. For cytochalasin-D experiments, cells were treated with 200 nM cytochalasin-D prior to uptake procedure for 20 min.

Magnetic Particle Quantification Within Cells

In order to correlate the percent uptake of particles to the number of particles internalized per cell, magnetic nanoparticle cell suspensions were added to a confluent culture of bovine aortic endothelial cells, which were further exposed to a magnetic field (LifeSep 96F, Dexter Magnetic Technologies) for 12 h. Then, the cells were rinsed three times with PBS, trypsinized and collected in Eppendorf tubes. Control cells (not loaded with magnetic particles) were counted in each well by using a hemocytometer and confirmed with a Coulter counter to estimate the total cell density per well. Eppendorf tubes containing magnetically loaded cells were then centrifuged, and the remaining pellet was digested with RIPA cell lysis buffer (Thermo Fisher Scientific, Rockford, IL, USA). After the centrifugation step, the magnetite content was determined spectrophotometrically (using Synergy^{TM} 4 plate reader, BioTek Instruments Inc., and UV compatible 96- well plates, BD Bioscienses) in 1N hydrochloric acid (λ=335 nm) against a standard curve after MNP degradation with 1N aqueous sodium hydroxide (90°C, 30 min) and dissolution of the iron containing precipitate in the acid solution (8,11,33). The magnetite content was correlated to the theoretical magnetite content in each particle type in order to determine the approximate number of particles internalized per single cell. Alternatively, magnetite content within cells was determined by measuring magnetic moment of the MNP-loaded (for 12 h) cells against a standard curve plotted by measuring magnetic moments of known amounts of MNP using an alternating gradient magnetometer (Princeton Instruments Corporation). MNP

containing cells were trypsinized, separated by centrifugation, re-suspended in 10 μL of PBS, deposited on 5 mm round glass slides, dried overnight and measured.

2-D Migration Studies

Bovine aortic endothelial cells were seeded on gridded cover slips from Electron Microscopy Sciences (Hatfield, PA, USA) with the aid of a cloning ring (VWR, Radnor, PA, USA). The cloning ring was placed in the center of the gridded cover slip, and cells were seeded in the interior of the cloning cylinder. Cells were allowed to reach confluence, and then the cell culture media inside the cloning cylinder was replaced with 100 μL of magnetic nanoparticle suspension. A 96-well magnetic separator (LifeSep 96F, Dexter Magnetic Technologies) was used to load magnetic nanoparticles within cells. After 12 h of cell loading on the magnet, the cloning ring was removed and cells were rinsed three times with PBS before beginning the migration assay. This process yielded a circle shaped area of magnetically loaded endothelial cells. Migration of the cells was measured by using light microscopy with the gridded coverslip to measure the distance cells traveled over a 45 h time period.

3-D Migration Studies

Fluoroblok transwell inserts were coated with 100 μg/mL type-I collagen from Sigma-Aldrich (St. Louis, MO, USA) for one hour and then rinsed with PBS. BAECs were loaded with 50% (w/w) magnetite containing MNPs for 12 h using a 96-well magnetic separator (LifeSep 96F, Dexter Magnetic Technologies). Control (not loaded) cells and magnetically loaded cells were then tryspinized and seeded in 5% FBS supplemented DMEM in the apical chamber of a 24-well Fluoroblok transwell insert. The basal section of the transwell insert contained DMEM supplemented with either 5% or 10% FBS. The 10% FBS in the bottom chamber was used to induce cell migration due to chemotaxis through the collagen coated membrane. Control cells and magnetically loaded cells were then allowed to migrate in each serum condition and either in a control condition (no field) or one with a static magnetic field from a NeFeB magnet ($50 \times 50 \times 12$ mm with an average z-direction field gradient of ~10 T/m and average surface field of 0.3 T). After 12 and 24 h of migration, the basal section of the well was aspirated and Calcein Green was applied to stain cells. Fluorescent images were then taken to determine the extent of migration that occurred in each well. Further, magnified images were taken at four random locations in order to quantify the number of cells that had migrated through the membrane.

Statistics

Experimental data presented in figures demonstrated the mean ± standard deviation. One-tailed, unequal variance *t*-tests were used to analyze the significance of MNP uptake and migration distances of various MNP-loaded and unloaded cells. A linear regression was used to demonstrate the rate of migration (in 2D experiment) of control and MNP loaded cells and determine whether there was a significant increase in BAEC migration rate between loaded and unloaded cells. In 3D migration experiments, two-way ANOVA was run for comparisons of multiple groups. In all tests, the differences were termed significant at $p<0.05$ and the degree of significance is given in figures when appropriate (* $p<0.05$; ** $p<0.01$; *** $p<0.001$). All statistics were performed via Graph Pad Prism (Graph Pad Software Inc., USA).

RESULTS

MNP Formulation

Magnetic nanoparticles were synthesized with magnetite concentrations of 11.5%, 28.1% and 46% (w/w) termed as ~10%, ~30% and ~50% magnetite loaded MNP respectively. The magnetite entrapment yield was found to be 93–95% for all formulations. The MNPs hydrodynamic diameters ranged between 277 and 301 nm for different magnetite loadings (by the dynamic light scattering). Size distribution was unaffected by varying magnetite entrapment. Zeta potentials indicating the MNPs surface charge were slightly negative and varied between −4.35 and −6.98 mV (Table I).

Magnetic Nanoparticle Uptake

The uptake of PLA-based magnetic nanoparticles loaded with 10%, 30% and 50% (w/w) iron oxide (magnetite) was quantitatively determined by measuring fluorescence of the internalized MNP fraction in the presence or absence of a static magnetic field. It is noteworthy to mention that higher loads of magnetite resulted in fluorescence quenching of the labeled PLA. However, since the fluorescence of internalized MNPs at each time point was normalized to the total fluorescence of each MNP type, quenching did not affect the calculation of the MNP percentage uptake. Figure 1a shows that the uptake of 50% loaded MNP into Bovine Aortic Endothelial Cells (BAECs) occurred with a quite rapid initial rate of ~$20\%_{uptake}$/hour for the first four hours almost reaching a saturation (subsequent uptake rate ~$0.6\%_{uptake}$/hour) at approximately 80% uptake of the given MNP dose. The initial uptake rates for 30%

Table I Characteristics of the PLA-Based Magnetic Nanoparticles (MNP) Stabilized with Polyvinyl alcohol (PVA) and Loaded with Theoretical 10%, 30% and 50% (w/w) Magnetite

Formulation description theoretical% (w/w) magnetite	Magnetite entrapment yield,%	Magnetite loading, % (w/w)	ζ-potential (mV)	MNP mean size (nm)[a]
12.2% (~10%)	94	11.5 ± 0.98	−5.24 ± 0.37	280
29.6% (~30%)	95	28.1 ± 1.19	−6.98 ± 0.51	301
49.5% (~50%)	93	46.0 ± 1.08	−4.35 ± 0.27	277

[a] Polydispersity index (PDI) of the MNP in all formulations was found to be in the range 0.17–0.20

and 10% loaded particles were found to be comparable ($p>0.1$) at about $10.5\%_{uptake}$/hour and $8.7\%_{uptake}$/hour respectively (based on the first eight hours) and were significantly ($p<0.005$) slower relative to 50% loaded MNPs. At ten hours, 30% loaded MNPs reached similar uptake percentage to that of 50% loaded MNPs and continued at the same rate for the rest of the observation period, reaching a maximum uptake of 91% and 87% (for 50% and 30% loaded MNP, respectively) after 24 h. In contrast, the uptake of 10% loaded MNPs remained well below 30% and 50% loaded MNPs from 6 h on ($p<0.0001$), reaching a maximum uptake of ~60% after the 24 h observation period (Fig. 1a). The control MNP uptake experiment without exposure to a magnetic field resulted in a significantly ($p<0.0001$) smaller internalization of MNPs within cells for particles of all magnetite loadings (Fig. 1b). We observed a direct correlation between the initial uptake rates and magnetite loadings resulting in maximal internalization of MNPs at about 31%, 25% and 11% for the 50%, 30% and 10% loaded MNPs respectively. When dilutions (0.75, 0.5 and 0.25 of the maximal MNP dose) were used in uptake experiments for 30% and 50% MNPs, the uptake efficiency after 24 h was reaching about 100% as compared to the 87 and 91% for the 30% and 50% MNP respectively at a maximal dose (not shown).

The applied force due to the presence of the magnetic field would be expected to enhance the sedimentation rate of the MNP and potentially help to overcome steric hindrance that would prevent direct interaction with cell surface receptors. To investigate whether the enhanced uptake is due to only to facilitation of the initial MNP

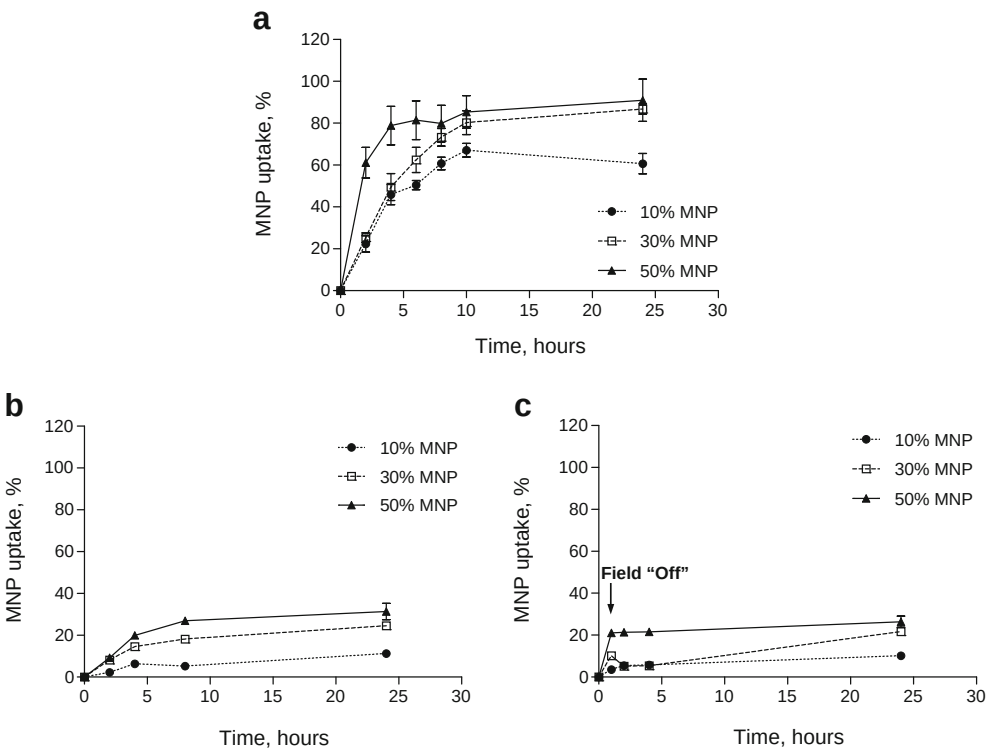

Fig. 1 The kinetics of 10%, 30% and 50% (w/w) MNP uptake by Bovine Aortic Endothelial Cells (BAECs) in culture as a function of incubation time and various magnetic field conditions. (**a**) A Magnetic field of 500 Gauss "On" by using a fixed magnet applied directly to the underside of the cell culture plates. (**b**) Magnetic field "Off". (**c**) Magnetic field on for 1 h then "Off". The MNP uptake was determined by fluorescence of internalized MNPs.

interaction with the cell or requires the continuous presence of the field, we performed uptake experiments in which the exposure of cells and particles to the magnet was discontinued after the first hour. The results of this experiment show that after the cells are removed from a magnet, MNP uptake is arrested, indicating that the continued application of force is required for enhanced particle internalization, Fig. 1c. It is noteworthy to mention that in the absence of the magnetic field (per Fig. 1b & c), there appears to be a limit to the number of particles that can be internalized despite the continuous availability of particles at the cell surface.

To determine whether or not MNP uptake was an active or passive process, cells were treated with 200 nM of cytochalasin-D, which is a cell permeable inhibitor of actin polymerization resulting in inhibition of phagocytosis. This dose was sufficient to observe slight deformation of cells, but did not initiate cell detachment or death. Cytochalasin-D treatment significantly decreased the ability of BAECs to internalize MNPs both with and without a magnetic field. BAECs treated with cytochalasin-D with no exposure to a magnetic field experienced 2.8, 2.8 and 3.6 times less MNP uptake for 10%, 30% and 50% MNPs respectively as compared to their non-treated counterparts. Cells treated with cytochalasin-D and exposed to a magnetic field experienced 10.0, 5.0 and 4.3 times less MNP uptake for 10%, 30% and 50% MNPs respectively as compared to their non-treated counterparts.

Cell Viability and Proliferation

Live cell staining was performed using CellTrace^{TM} Calcein Green AM reagent. In live cells, the nonfluorescent CellTrace Calcein Green AM is converted to a green-fluorescent Calcein after intracellular esterases remove the acetoxymethyl (AM) esters. The magnetic nanoparticles were internalized within the cells on a magnet for 12 h. Live cells were stained green (488/530 nm), while magnetic nanoparticles exhibited red fluorescence (588/617 nm). Figure 2 shows no significant differences in cell viability for all magnetite loadings comparing to the control cells not treated with MNPs.

To further examine MNP compatibility within cells, we utilized the Alamar Blue assay 48 h after the conclusion of magnetic nanoparticle incubation. The MNP uptake was conducted for 12 h using various dilutions of MNPs. Figure 3 shows that a maximum of 15% in fluorescence variation relative to control cells was measured for particles of all loadings at different dilutions. The maximum dose used in these experiments showed 84±12% survival for 10% loaded MNPs, 85±1% survival for 30% loaded MNP and 88±2% for 50% loaded MNP.

In the cell proliferation experiment, a confluent culture of BAECs was loaded with 10, 30 and 50% MNPs for 8 h to obtain various MNP contents within cells (based on the uptake kinetics per Fig. 1a). Non-loaded cells were used as a control. Subsequently all cell groups were trypsinized and re-seeded at a dilution of 1:6 to quantify cell proliferation

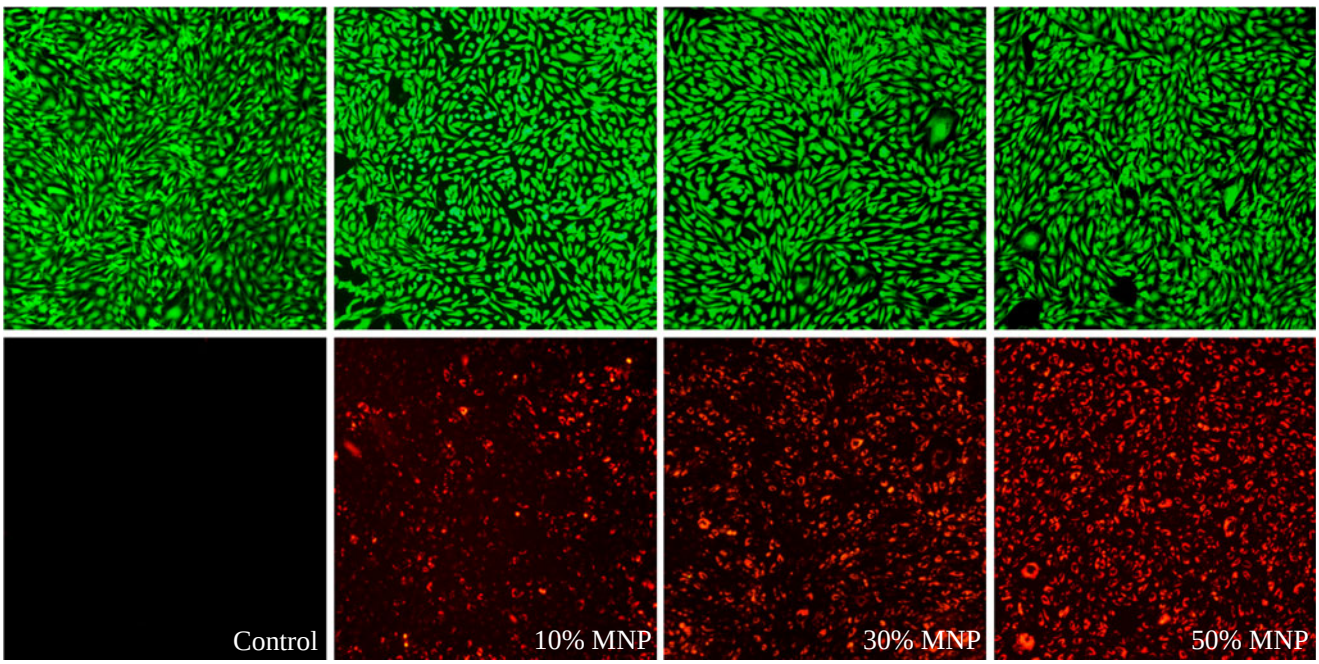

Fig. 2 Micrographs of Bovine Aortic Endothelial Cells (BAECs) in green and red fluorescent channels qualitatively showing the relative amount of 10%, 30% and 50% magnetite loaded MNPs internalized within cells at 12 h time point. Control cells were not treated with MNPs. Green fluorescent micrographs show healthy cells as assessed by Calcein Green staining. (Magnification: x100).

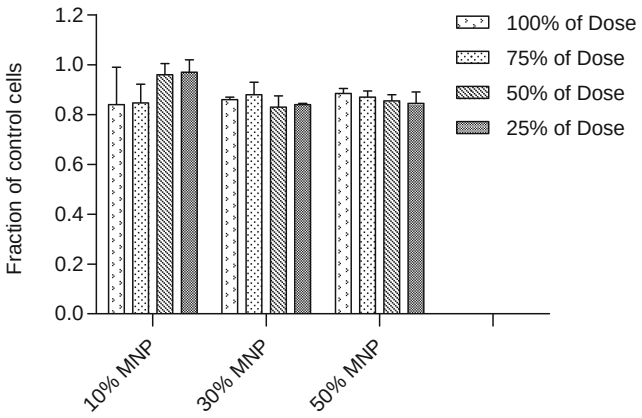

Fig. 3 Alamar Blue assay for Bovine Aortic Endothelial cells (BAECs) loaded for 12 h with 10%, 30% and 50% MNPs and various dilutions. The Alamar Blue assay was performed 48 h post loading with MNPs. Cell survival is presented as a fraction relatively to control, unloaded cells. There was no statistically significant difference within each group and between the groups.

rates using Alamar Blue assay. Figure 4 shows that all cells either loaded or non-loaded with particles proliferated with an identical rate during the 3 days cultivated in 10% FBS supplemented DMEM medium.

Magnetic Particle Quantification

The amount of magnetite uptake into cells was found by spectrophotometry measuring specific absorption of iron at 335 nm as previously described (33). At a 12 h time point the amount of magnetite internalized by the cells that were loaded with 10%, 30% and 50% MNPs was found to be 2.7±0.9 pg/cell, 10.4±2.4 pg/cell and 26.3±4.7 pg/cell respectively. According to magnetometry, the amount of magnetite uptake into cells was found to be 8.3±1.7 pg/cell and 23±1.0 pg/cell for 30% and 50% MNPs respectively. The estimation of 10% MNP loading within cells by magnetometry was below the limit of detection of this method. The saturation magnetic moment for cells loaded with 30% and 50% MNPs was found to be ~150 and ~400 nemu/cell respectively (Fig. 5). The values of magnetite content within BAECs were similar to previously reported iron oxide contents achieved in $CD133^+$ human stem cells (9.5 pg/cell) (34), human mesenchymal stem cells (MSCs) (11 pg/cell) and hematopoietic ($CD34^+$) stem cells (2 pg/cell) (35). Using the magnetite content of the particles and the MNP geometry (assuming an average MNP diameter of 300 nm, (11,33)), the number of magnetic nanoparticles incorporated into a single cell could be estimated. Cells loaded with 10%, 30% and 50% MNPs for 12 h were found to have accumulated approximately 2,000 MNPs/cell, 2,300 MNPs/cell and 2,600 MNPs/cell respectively. Therefore, MNPs incorporated into a single cell took up approximately 5%, 6% and 7% of the cell's total volume, respectively.

Migration Studies

2-D migration studies were performed without the influence of a magnetic field to determine whether the presence of magnetic nanoparticles in the cytoplasm would impair the dynamic reorganization of the cytoskeleton required for cell motility. Images of cells in a 2-D migration assay were taken *via* light microscope, and image analysis was used to quantify the distance traveled by the leading edge of

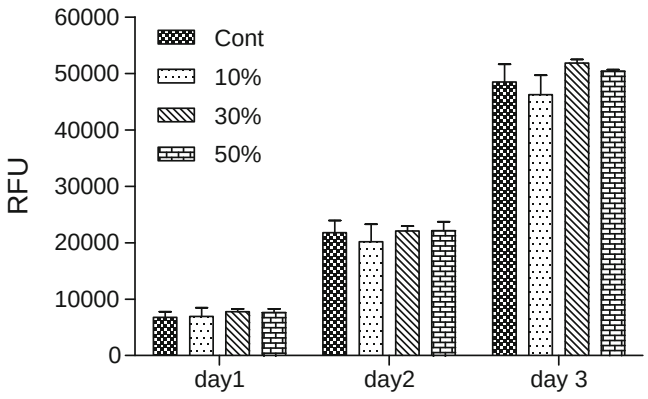

Fig. 4 MNP-loaded cell proliferation experiment. Bovine aortic endothelial cells loaded with 10%, 30% and 50% MNPs for 8 h, were trypsinized and re-seeded at a density of 1:6 relative to the original confluent culture. Non loaded cells used as a control. Cell proliferation rates were quantified by the Alamar Blue assay. All cells either loaded or non-loaded with particles proliferated with an identical rate during the 3 days cultivated in 10% FBS supplemented DMEM medium.

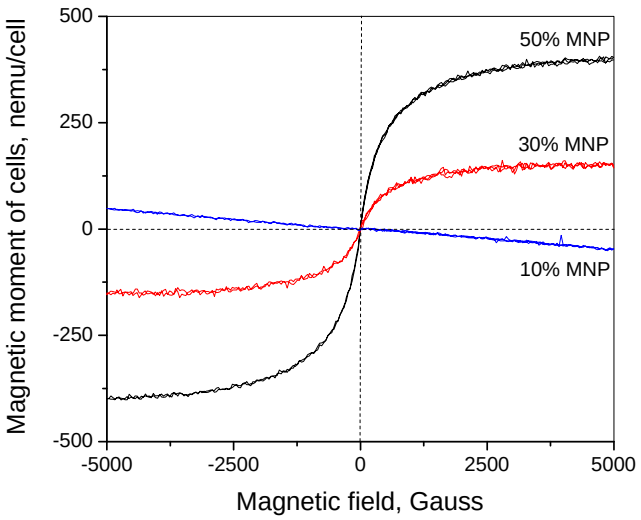

Fig. 5 Magnetic behavior of MNP-laden bovine aortic endothelial cells loaded for 12 h with 10%, 30% and 50% (w/w) magnetite containing MNP.

the cell monolayer. Migration distance was statistically different ($p<0.05$) from the control for cells loaded for 12 h with 10%, 30% or 50% MNPs (Fig. 6). However, the difference was not inhibitory. An increase in MNP loadings led to an increase in migration distance or rate. 3-D Migration studies utilized 50% MNP loading into cells since these particles experienced the strongest magnetic forces and resulted in maximal cell loading that we could obtain per time period. Migration rates were determined by measuring fluorescence intensity of the cells that had migrated to the bottom side of the Fluoroblok wells, which block the fluorescence of cells located on top of the membrane. FBS concentration differences (5% *vs.* 10%) in appical and basal chambers (FBS gradient) were used as a positive control for chemotactically stimulated cell migration. Figure 7 demonstrates that migration of MNP-loaded cells in the absence of a magnetic field is not significantly different from unloaded control cells, with or without a gradient in FBS ($p>0.6$). However, with no FBS gradient, the migration of MNP-loaded cells in the presence of a magnetic field was approximately 2.5 times greater than unloaded control cells ($p<0.001$) and was comparable to migration rates due to an FBS gradient. In the presence of an FBS gradient, the addition of a magnetic field further increased the migration rate 1.2 fold ($p=0.01$) compared to MNP-loaded cells without a field. To be certain that these were migratory effects and not effects of increased proliferation as a result of MNP loading, Alamar Blue staining was performed at 12 h and 24 h time points. Alamar Blue at the 24 h time point indicated that there were ~125,000 cells/trans-well for wells that did not show a FBS concentration gradient and ~135,000 cells/trans-well for well that did show a FBS concentration gradient. These values both correlate well with the 0.5 population doublings/day in 5% supplemented FBS DMEM that is suggested for bovine aortic endothelial cells (36). There was not however

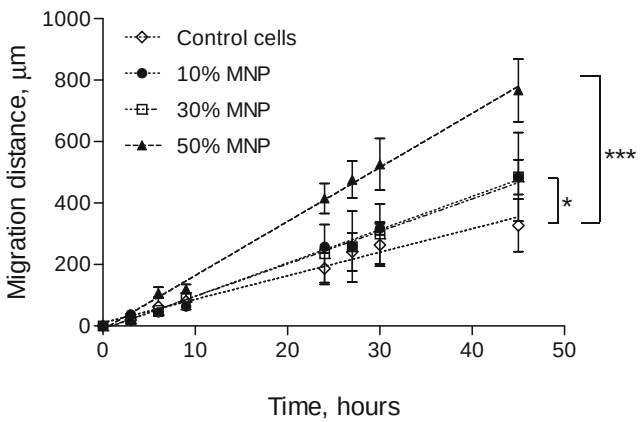

Fig. 6 Two dimensional cell migration experiment. Migration distance and rate of migration was increased in BAEC cells loaded with 10%, 30% and 50% MNPs for 12 h in comparison to control cells. Loaded cells migrated at a statistically higher rate than that of control cells.

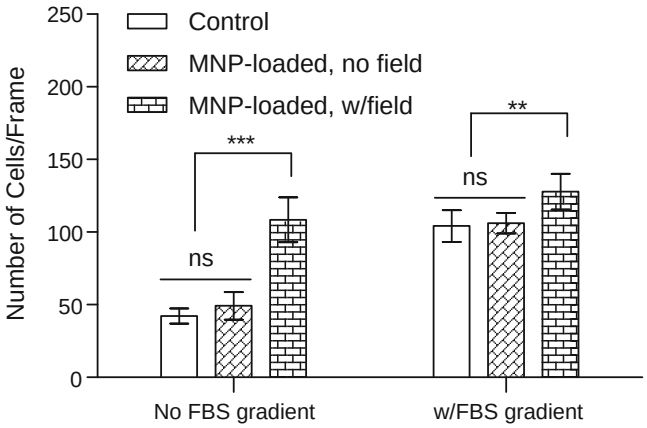

Fig. 7 BAEC cells were loaded with 50% MNPs for 12 h before being placed into a Transwell insert for 3-D migration. A 24 h time point migration was measured under the influence of a static magnetic field and without the influence of a magnetic field for loaded cells and compared to control, unloaded cells. An increase in FBS concentration in the basal chamber (FBS gradient) of the trans-wells was used as a positive control for each experimental condition. A 12 h time point migration exhibited similar pattern to 24 h time point.

an increase in cell number between magnetically loaded and non-loaded cells, indicating that the enhanced migration was not an effect of the increase in cell proliferation.

DISCUSSION

The aims of this study were to evaluate the effects of magnetic forces acting on cells with respect to the MNP internalization kinetics and mechanism and to determine if the MNP uptake into cells is a force dependent process. We also wished to assess how cells tolerate high doses of MNPs and whether the high MNP loads would interfere with cellular functions. This information is of high relevance for magnetically-mediated cell targeting applications in which the responsiveness of MNPs is an important parameter to allow efficient targeting. In addition, the cytocompatibility of MNPs is a very important prerequisite in magnetic cell targeting applications because targeted cells are expected to provide a therapeutic effect at the target site, either by restoration of a physiologically normal cellular layer e.g. in stent applications (37) or by secreting regulatory factors or "drugs" utilizing cellular machinery mechanisms (38). To understand how magnetic forces affect MNP uptake kinetics and internalization mechanism, we formulated magnetic nanoparticles of distinctive theoretical magnetite loads of 10%, 30% and 50% (w/w). The efficiency of magnetite incorporation was about 93–95% for all formulations. These high magnetite incorporation efficiencies indicate a consistent level of magnetic material loading matching well the expected theoretical values. Particles of all loads exhibited a mean hydrodynamic diameter in a range

277–301 nm, which indicates that magnetite loadings did not affect particle size.

Because magnetic force is proportional to the magnetic moment of particles, we would expect that the force exerted on an endothelial cell by a MNP exposed to a magnetic field will increase as magnetite concentration within the particle rises. Our results show that 277–301 nm MNPs internalize within endothelial cells exposed to a magnetic field at different rates, depending on the magnetite incorporation per particle (Fig. 1a). This indicates that the uptake mechanism used by the cell is force dependent. Our results further indicate that MNPs are also taken into the cell without the influence of a magnetic field, but to a lesser extent. It was therefore important to examine if the magnetic field actually stimulates uptake because of the force it is applying on a cell, or whether it just allows the MNPs to reach a surface of the cell at a faster rate. To examine this phenomenon, we conducted an experiment where MNPs given to cells were exposed to a magnet for only one hour (a sufficient time to sediment >90% of MNPs). We found that before removal of the magnet (1 h time point), the MNP uptake rates were similar to those seen in previous magnetic experiments; however, after the removal of the magnet, MNP uptake was stalled, and there was minimal additional uptake for the remainder of the observation period. This result also supports the idea that MNP uptake is a force-dependent process and not an effect of the magnetic field causing more rapid delivery of MNPs to the cell-surface or enhancing the initial interaction between the particles and the cell surface. No further increase in MNP uptake after removal of the magnet at a 1 h time point shows that internalization of a fraction of MNPs (21%, 10% and 4% uptake for 50%, 30% and 10% loaded particles respectively, Fig. 1a) cause cells to reach saturation with no additional ability to internalize more particles. These levels of uptake correlate well with the final uptake extents in the non-magnetic uptake experiment (Fig. 1b). This observation demonstrates that, in the absence of a magnetic field, the cells' ability to internalize particles is limited; however, when magnetic field is applied, the sustained magnetic force will cause internalization of nearly the full dose of MNPs.

While our results indicate that MNP uptake is a force-dependent process, we also performed tests to determine whether uptake was an active process involving the actin cytoskeleton or a passive, force-driven deformation of cellular structures. BAECs were treated with 200 nM cytochalasin-D in order to depolymerize actin filaments and inhibit their active reorganization within the cells' cytoskeleton. This in turn, inhibits phagocytosis, an endocytotic mechanism that is highly dependent on cytoskeletal reorganization and actin polymerization. If MNP uptake were happening via a passive deformation process, we would expect treatment of BAECs with cytochalasin-D to increase MNP internalization due to the cell being both less stiff and strong. However, our results showed that MNP uptake into BAECs cells was completely inhibited after cells were treated with cytochalasin-D. This suggests that the process of MNP uptake in the presence of a magnetic field is an active process, requiring actin remodeling.

To estimate the approximate number of magnetic nanoparticles present in a single cell, we utilized the known mean diameter of MNPs as well as magnetite content information obtained after loading in conjunction with the theoretical values we would obtain from the chemical equations and protocol of MNP formulation. We found that after 12 h of loading, 10%, 30% and 50% MNPs comprised approximately 5%, 6% and 7% of the entire endothelial cell volume respectively. This value can be considered a lower limit given the assumptions made throughout the quantification process.

To determine the health status of MNP-loaded cells, we stained cells with the cell-permeant dye, Calcein Green. The images of BAEC fully-loaded with MNPs exhibit the same cell density and morphology as control cells not loaded with particles. Fluorescent images of the MNPs internalized within cells after 12 h correspond well with the fluorescent uptake data found in the uptake experiments, and Calcein Green staining indicates viability of the cells. Alamar Blue, whose fluorescence depends on cellular respiration, was used as an additional measure of cell viability. Cells loaded with 10% MNPs diluted to 25% and 50% show viability above 95% in comparison to control. All other MNP loadings and dilutions showed viability of 85% in comparison to control. Overall, Alamar Blue results were in agreement with Calcein Green images of the cells. These results indicate that, for 48 h post uptake, cells maintain their healthy state showing a very marginal decrease in viable cell number.

Although preliminary viability tests indicate relatively healthy cells after loading with MNPs, an important characteristic of magnetically loaded endothelial cells for drug delivery or targeting would be the ability to utilize them as one would non-loaded cells. That means that we would expect MNP-loaded cells to proliferate after delivery with a comparable rate to non-loaded cells. To confirm that MNP loading doesn't impair cellular ability to divide, BAECs loaded with 10%, 30% and 50% MNPs for 8 h (resulting in a range of MNP internalization contents, see Fig. 1a) were trypsinized and reseeded at a lower (1:6 of the original) cell density. Our results clearly demonstrate that MNP-loaded cells proliferate identically to control cells division rate of one division per 24 h during 3 days in 10% FBS supplemented DMEM, indicating that MNP-loaded cells preserve their ability to divide despite the high content of MNPs within cells.

It was expected that the high loading of MNPs exhibited after 12 h of MNP uptake into BAECs would affect the ability for cells to migrate over a flat surface; however, our results showed that MNP uptake into cells significantly increased rate of cell migration for 10% ($p<0.05$), 30% ($p<0.05$) and 50% ($p<0.0001$) in comparison to control cells. The increase in migration rate with MNP loading can potentially be described in a few ways, with further research necessary to fully elucidate the actual mechanism. Previous work has suggested that MNP incorporation into endothelial cells causes intercellular gaps to form (39). Given that BAEC growth and migration is contact inhibited, an increase in intercellular gap distance, by either shrinkage of the cell or some other method, would signal for the cell to grow and/or migrate. Our loaded cells do exhibit a slight shrinkage as seen in the Fig. 2 that could be the cause of the observed increase in migration of cells. Similarly, uptake of similarly sized MNPs has been reported to decrease intercellular gap junction communication (40). This work found that stress kinases and β-catenin levels modulate the alterations in intercellular gap junction communication. This suggests that the exposure of cells to MNPs induces a stress response that leads to a down regulation of intercellular signaling. Thus, MNP-induced loss of cell contact and gap junctional communication may explain, in part, the observed increase in motility; however, it is not clear if this is a transient or chronic response. We did not observe an increase in proliferation over the course of the migration experiments, and our data on viability and proliferation suggest that the MNP-loaded cells do not exhibit abnormal growth long term as might be expected with a prolonged loss of contact inhibition. In terms of the effect of the presence of MNPs on cytoskeletal dynamics, it appears that MNP loading does not inhibit cell motility.

MNP-loaded cells have been targeted *in vitro* to tissues for cell attachment (41) and even to implants (17,42). However, the potential of MNP-loaded cells as targeted cell delivery/targeting vectors can be enhanced if we can characterize and manipulate their movement through tissues. As a first step in order to eliminate the idiosyncrasies of transport through soft tissues, it is necessary to determine how MNP-loaded endothelial cells can navigate through a membrane with or without an applied magnetic field. Our 3-D migration experiments of MNP-loaded endothelial cells through a transwell membrane show that not only are maximally loaded 50% MNP-loaded cells capable of migrating, but there is a significant ($p<0.001$) increase in migration of MNP-loaded endothelial cells under the influence of a magnetic field. In the absence of a magnetic field, the transmigration of MNP-loaded cells was no different ($p>0.05$) from control cells with or without a gradient in FBS, indicating that the presence of MNPs does not impair the migratory response of these cells. MNP-loaded endothelial cells exposed to a magnet without an FBS gradient exhibited a dramatic increase in migration that was the same magnitude ($p>0.05$) as the effect of adding an FBS gradient on the migratory patterns of control cells. In the presence of an FBS gradient, the application of a field resulted in an additional 20% increase in migration of the MNP-loaded cells, while cell proliferation assay, Alamar Blue, showed that the enhanced migration was not an effect of the increase in cell number. These results suggest that the magnetic force does in fact encourage a migratory response in MNP-loaded cells. Overall, these results are promising indicators that magnetically loaded cells have great potential as targeted therapy delivery vectors and that magnetic fields can be used to facilitate migration into tissues.

CONCLUSION

Biodegradable MNPs were formulated with variable loading of magnetite in a range of 10–50% (w/w). A neodymium magnet placed below the cell culture plate creates a magnetic field gradient generating forces on the particles proportional to the magnetite content. The internalization rate of MNPs by endothelial cells is dependent upon the magnetite loading within particles, indicating that uptake is a force-dependent process. Furthermore, the degree of internalization in the absence of a magnetic field or with a field for only the first hour after MNP were introduced to the cells was dramatically reduced. MNP-loading of cells did not impair cellular ability to proliferate compared to control non-loaded cells. Two dimensional migration studies indicate cytoskeletal functions are still intact, despite high MNP loading of cells. Both two- and three-dimensional migration studies showed that cell motility is not impaired despite the inclusion of MNPs of up to 7% the volume of the cell. Finally, application of a magnetic field during the three dimensional migration enhanced migration of MNP loaded cells to the same extent as a chemotactic stimulus. While more investigation is needed to fully elucidate the effect of MNPs on sub-cellular organelle functions, it appears that MNP loadings do not impair either the proliferative capacity or migratory behavior of the cells.

ACKNOWLEDGMENTS & DISCLOSURES

This study was partially supported by Award Number R01HL107771 from the National Heart, Lung, And Blood Institute and by Award Number F31 GM086128-01 from National Institute of General Medical Sciences supporting Cristin MacDonald's PhD program through Ruth Kirschstein Research Service Award (RSA). The content is solely the responsibility of the authors and does not necessarily represent the official views of the "National Heart, Lung, And Blood

Institute or the National Institutes of Health." Authors thank Dr. Robert Levy from the Children's Hospital of Philadelphia for his generous gift of the poly(lactide) covalently labeled with BODIPY® 564/570 (Life Technologies™) and Richard Sensenig from the Department of Surgery, Drexel University College of Medicine for reviewing the manuscript and providing constructive suggestions.

REFERENCES

1. McBain S, Yiu HH, Dobson J. Magnetic nanoparticles for drug and gene delivery. Int J Nanomed. 2008;3:169–80.
2. Pankhurst QA, Thanh NKT, Jones SK, Dobson J. Progress in applications of magnetic nanoparticles in biomedicine. J Phys D Appl Phys. 2009;42.
3. Polyak B, Friedman G. Magnetic targeting for site-specific drug delivery: applications and clinical potential. Exp Opin Drug Deliv. 2009;6:53–70.
4. Plank C, Schillinger U, Brill T, Rudolph C, Huth S, Gersting S, Krotz F, Hirschberger J, Bergemann C. Advances in magnetofection—magnetically guided nucleic acid delivery. J Magn Magn Mater. 2005;293:501–8.
5. Mykhaylyk O, Zelphati O, Rosenecker J, Plank C. siRNA delivery by magnetofection. Curr Opin Mol Ther. 2008;10:493–505.
6. Chariand D, Pickard M. Enhancement of magnetic nanoparticle-mediated gene transfer to astrocytes by 'magnetofection': effects of static and oscillating fields. Nanomedicine. 2010;5:217–32.
7. Dobson J, McBain SC, Farrow N, Batich CD. Magnetic nanoparticle-based gene trasnfection using oscillating magnet arrays. Tissue Eng Part A. 2008;14:875–6.
8. Chorny M, Fishbein I, Alferiev I, Levy RJ. Magnetically responsive biodegradable nanoparticles enhance adenoviral gene transfer in cultured smooth muscle and endothelial cells. Mol Pharm. 2009;6:1380–7.
9. Chorny M, Polyak B, Alferiev IS, Walsh K, Friedman G, Levy RJ. Magnetically driven plasmid DNA delivery with biodegradable polymeric nanoparticles. FASEB J. 2007;21:2510–9.
10. Mah C, Fraites Jr TJ, Zolotukhin I, Song S, Flotte TR, Dobson J, Batich C, Byrne BJ. Improved method of recombinant AAV2 delivery for systemic targeted gene therapy. Mol Ther. 2002;6:106–12.
11. Johnson B, Toland B, Chokshi R, Mochalin V, Koutzaki S, Polyak B. Magnetically responsive, paclitaxel-loaded biodegradable nanoparticles for treatment of vascular disease: preparation, characterizaton and *in vitro* evaluation of anti-proliferative potential. Curr Drug Deliv. 2010;7:263–73.
12. Senyei A, Widder K, Czerlinski G. Magnetic guidance of drug-carrying microspheres. J Appl Phys. 1978;49:3578–83.
13. Lubbe AS, Alexiou C, Bergemann C. Clinical applications of magnetic drug targeting. J Surg Res. 2001;95:200–6.
14. Jain TK, Morales MA, Sahoo SK, Leslie-Pelecky DL, Labhasetwar V. Iron oxide nanoparticles for sustained delivery of anticancer agents. Mol Pharm. 2005;2:194–205.
15. Hafeli UO, Riffle JS, Harris-Shekhawat L, Carmichael-Baranauskas A, Mark F, Dailey JP, Bardenstein D. Cell uptake and *in vitro* toxicity of magnetic nanoparticles suitable for drug delivery. Mol Pharm. 2009;6:1417–28.
16. Muthana M, Scott SD, Farrow N, Morrow F, Murdoch C, Grubb S, Brown N, Dobson J, Lewis CE. A novel magnetic approach to enhance the efficacy of cell-based gene therapies. Gene Ther. 2008;15:902–10.
17. Polyak B, Fishbein I, Chorny M, Alferiev I, Williams D, Yellen B, Friedman G. High field gradient targeting of magnetic nanoparticle-loaded endothelial cells to the surfaces of steel stents. PNAS. 2008;105:698–703.
18. Pislaru SV, Harbuzariu A, Agarwal G, Witt T, Gulati R, Sandhu NP, Mueske C, Kalra M, Simari RD, Sandhu GS. Magnetic forces enable rapid endothelialization of synthetic vascular grafts. Circulation. 2006;114:I314–318.
19. Pislaru SV, Harbuzariu A, Gulati R, Witt T, Sandhu NP, Simari RD, Sandhu GS. Magnetically targeted endothelial cell localization in stented vessels. J Am Coll Cardiol. 2006;48:1839–45.
20. Mornet S, Vasseur S, Grasset F, Duguet E. Magnetic nanoparticle design for medical diagnosis and therapy. J Mater Chem. 2004;14:2161–75.
21. Gupta AK, Gupta M. Synthesis and surface engineering of iron oxide nanoparticles for biomedical applications. Biomaterials. 2005;26:3995–4021.
22. Cinti C, Taranta M, Naldi I, Grimaldi S. Newly engineered magnetic erythrocytes for sustained and targeted delivery of anti-cancer therapeutic compounds. PLoS One. 2011;6.
23. Magnani A, Pierige F, Serafini S, Rossi L. Cell-based drug delivery. Adv Drug Deliv Rev. 2008;60:286–95.
24. Forbes ZG, Yellen BB, Halverson DS, Fridman G, Barbee KA, Friedman G. Validation of high gradient magnetic field based drug delivery to magnetizable implants under flow. IEEE Trans Biomed Eng. 2008;55:643–9.
25. Chorny M, Fishbein I, Yellen BB, Alferiev IS, Bakay M, Ganta S, Adamo R, Amiji M, Friedman G, Levy RJ. Targeting stents with local delivery of paclitaxel-loaded magnetic nanoparticles using uniform fields. Proc Natl Acad Sci USA. 2010;107:8346–51.
26. Kim J, Yoon T, Yu K, Noh M, Woo M, Kim B. Cellular uptake of magnetic nanoparticles is mediated through energy-dependent endocytosis in A549 cells. J Vet Sci. 2006;7.
27. Lunov O, Zablotskii V, Syrovets T, Rocker C, Tron K, Nienhaus GU, Simmet T. Modeling receptor-mediated endocytosis of polymer-functionalized iron oxide nanoparticles by human macrophages. Biomaterials. 2011;32:547–55.
28. Maand Y, Gu H. Study on the endocytosis and the internalization mechanism of aminosilane-coated Fe3O4 nanoparticles *in vitro*. J Mater Sci Mater Med. 2007;18:2145–9.
29. Wuang SC, Neoh KG, Kang ET, Pack DW, Leckband DE. HER-2-mediated endocytosis of magnetic nanospheres and the implications in cell targeting and particle magnetization. Biomaterials. 2008;29:2270–9.
30. Scherer F, Anton M, Schillinger U, Henkel J, Bergemann C, Kruger A, Gansbacher B, Plank C. Magnetofection: enhancing and targeting gene delivery by magnetic force *in vitro* and *in vivo*. Gene Ther. 2002;9:102–9.
31. Chari DM, Pickard MR, Barraud P. The transfection of multipotent neural precursor/stem cell transplant populations with magnetic nanoparticles. Biomaterials. 2011;32:2274–84.
32. Dobson J, McBain SC, Griesenbach U, Xenariou S, Keramane A, Batich CD, *et al*. Magnetic nanoparticles as gene delivery agents: enhanced transfection in the presence of oscillating magnet arrays. Nanotechnology. 2008;19.
33. MacDonald C, Friedman G, Alamia J, Barbee K, Polyak B. Time-varied magnetic field enhances transport of magnetic nanoparticles in viscous gel. Nanomedicine. 2010;5:65–76.
34. Gamarra LF, Pavon LF, Marti LC, Pontuschka WM, Mamani JB, Carneiro SM, Camargo-Mathias MI, Moreira-Filho CA, Amaro Jr E. *In vitro* study of CD133 human stem cells labeled with superparamagnetic iron oxide nanoparticles. Nanomedicine. 2008;4:330–9.
35. Arbab AS, Yocum GT, Kalish H, Jordan EK, Anderson SA, Khakoo AY, Read EJ, Frank JA. Efficient magnetic cell labeling with protamine sulfate complexed to ferumoxides for cellular MRI. Blood. 2004;104:1217–23.

36. Castellot JJ, Karnovsky MJ, Spiegelman BM. Potent stimulation of vascular endothelial cell-growth by differentiated 3t3 adipocytes. Proc Natl Acad Sci USA-Biol Sci. 1980;77:6007–11.
37. Ong AT, Aoki J, Kutryk MJ, Serruys PW. How to accelerate the endothelialization of stents. Arch Mal Coeur Vaiss. 2005;98:123–6.
38. Taha MF. Cell based-gene delivery approaches for the treatment of spinal cord injury and neurodegenerative disorders. Curr Stem Cell Res Ther. 5:23–36.
39. Apopa PL, Qian Y, Shao R, Guo NL, Schwegler-Berry D, Pacurari M, *et al.* Iron oxide nanoparticles induce human microvascular endothelial cell permeability through reactive oxygen species production and microtubule remodeling. Part Fibr Toxicol. 2009;6.
40. Ale-Agha N, Albrecht C, Klotza LO. Loss of gap junctional intercellular communication in rat lung epithelial cells exposed to carbon or silica-based nanoparticles. Biol Chem. 2010;391: 1333–9.
41. Patel S, Bachman LA, Hann CR, Bahler CK, Fautsch M. Human corneal endothelial cell transplantation in a human *ex vivo* model. Investig Ophthalmol Vis Sci. 2009;50:2123–31.
42. Forbes ZG, Barbee KA, Stoddard FR, Morgan DA, Brooks AD, Friedman G. Improving the efficacy of cellular therapy by magnetic cell targeting. Cytotherapy. 2006;8.